

# Computer-aided analysis of gait rhythm fluctuations in amyotrophic lateral sclerosis

Yunfeng Wu · Sridhar Krishnan

Received: 1 May 2009 / Accepted: 12 August 2009 / Published online: 26 August 2009  
© International Federation for Medical and Biological Engineering 2009

**Abstract** Deterioration of motor neurons due to amyotrophic lateral sclerosis (ALS) would affect the strides from one gait cycle to the next. Computer-assisted techniques are useful for gait analysis, and also have high potential in quantitatively monitoring the pathological progression. In this paper, we applied the signal turns count method to measure the fluctuations in the swing-interval time series recorded from 16 healthy control subjects and 13 patients with ALS. The swing-interval turns count (SWITC) parameter derived with the threshold of 0.06 s presented a significant difference ( $p < 0.001$ ) between the healthy control subjects and ALS patients. Besides the SWITC, we also computed the averaged stride interval (ASI), which is usually longer in the patient with ALS ( $p < 0.0001$ ), to characterize the gait patterns of ALS patients. In the pattern classification experiments, the Fisher's linear discriminant analysis (FLDA) and the least squares support vector machine (LS-SVM), both input with the SWITC and ASI features, were evaluated using the leave-one-out cross-validation method. The results showed that the LS-SVM with sigmoid kernels was able to provide a classification accurate rate of 89.66% and an area of 0.9629 under the receiver operating characteristic (ROC) curve, which were superior to those obtained with the linear classifier in the form of FLDA.

**Keywords** Gait analysis · Movement disorders · Amyotrophic lateral sclerosis · Pattern classification · Support vector machine · Rehabilitation engineering

## 1 Introduction

In the central nervous system of a human body, motor neurons are the nerve cells that process sensory information and control voluntary muscle movement [26]. Amyotrophic lateral sclerosis (ALS), which is also referred to as Lou Gehrig's disease, is a type of neurodegenerative disorder that primarily affects upper motor neurons in the brain and lower motor neurons connecting the brain stem and spinal cord to muscle fibers [3, 17]. The degenerative motor neurons are no longer able to send the impulses initiated by the brain to the muscle fibers, which affects normal body motions [5]. Furthermore, the motor neurons will be progressively replaced with fibrous astrocytes, and the muscle tissue gradually atrophies [19]. Early clinical symptoms of ALS often include twitching and cramping of the arms or legs, difficulty speaking or swallowing, or muscle fatigue [17, 29]. Patients with ALS at the advanced stages may become paralyzed [3].

Since flexion and extension motions of two lower limbs are regulated by the central nervous system, the gait of a patient with a neurodegenerative disorder would become abnormal due to deterioration of motor neurons. Previous studies [4, 8, 9, 11, 14, 15, 21] demonstrated that computer-aided analysis of gait patterns could help the neurologist better understand the mechanism of motor control in the human body, and is also useful for monitoring of progressive neurological diseases. The research group led by Akay, Tamura, and Fujimoto [1, 2, 27, 28] applied the wavelet-based fractal analysis and time-frequency matching pursuit algorithm to acceleration signals recorded during climbing stairs and walking along a corridor, in order to study the gait patterns related to neurodegenerative diseases. Their studies suggested that the acceleration signal from one gait cycle to the next would be altered into

Y. Wu (✉) · S. Krishnan  
Department of Electrical and Computer Engineering, Ryerson  
University, 350 Victoria Street, Toronto, ON M5B 2K3, Canada  
e-mail: y.wu@ieee.org

a more complex pattern with aging and with Parkinson's disease (PD), and the fractal dimensions of the body motion of patients with PD tend to be higher than those of healthy elderly subjects [2, 27]. Hausdorff et al. [13] estimated variations of gait cycle duration or stride interval (time from initial contact of one foot to the subsequent contact of the same foot) in neurological diseases. They used the detrended fluctuation analysis method to quantify the gait dynamics in ALS. The findings, in their study, can be summarized as follows [13]: (1) the average stride interval (ASI) of patients with ALS is significantly longer than that of healthy controls or of patients with PD or Huntington's disease (HD), (2) walking speed of patients with ALS is lower than that of healthy controls, but similar to that of patients with PD or HD, (3) the values of two measures of the fluctuation magnitude of stride interval in ALS, i.e., the coefficient of variation and standard deviation (SD) of the detrended stride-interval time series, are larger than those of healthy controls, similar to those of PD patients, and lower than those of HD patients, respectively, and (4) two measures of the temporal fluctuation dynamics, i.e., the fractal scaling index and normalized nonstationary index, are not significantly different from those observed in healthy controls.

Although an increase of stride interval was observed in ALS, there lacks evidence to demonstrate whether or not the swing interval (amount of time one foot is in the air), a subphase of stride interval, exhibits a higher degree of fluctuations in the patient with ALS, compared with that of a healthy subject. In order to measure the fluctuations of swing interval in ALS, we counted the number of significant signal turns in the swing-interval time series of patients with ALS. It is hypothesized that the swing interval turns count (SWITC) of the ALS patients might be different from that of healthy subjects, and the ALS gait patterns, characterized by the SWITC parameter and the known ASI feature, could be distinguished from the gait patterns of healthy subjects using the linear and nonlinear classifiers.

## 2 Methods

### 2.1 Gait assessment

#### 2.1.1 Subjects

The gait rhythm data used in the present study were provided by Hausdorff et al. [12], and can be downloaded via PhysioNet<sup>1</sup> [22]. Sixteen healthy control (CO)

subjects (2 men and 14 women) aged 20–74 years, with a mean age of  $39.3 \pm 18.5$  (mean  $\pm$  SD) years, were asked to participate. Thirteen ALS subjects (10 men and 3 women) aged 36–70 years, with a mean age of  $55.6 \pm 12.8$  years, were recruited from the Neurology Outpatient Clinic at Massachusetts General Hospital, Boston, MA, USA. The duration of the ALS subjects, since the pathological diagnosis ranged from 1 to 54 months, with a mean of  $18.3 \pm 17.8$  months, and the medication usage for each ALS subject was not changed. These ALS subjects did not usually use a wheelchair for mobility, and were free of other pathologies that might affect the gait. The presence or absence of symptoms that might affect lower extremity weakness was identified by clinical examinations.

#### 2.1.2 Experimental protocol

Each subject provided informed consent as approved by the Institutional Review Board of the Massachusetts General Hospital. According to the experimental protocol [12], each subject was requested to walk at his or her normal pace along a straight hallway of 77 m in length for 5 min (300 s). The force applied to the ground for each stride was recorded using ultrathin force-sensitive switches placed inside each subject's shoes and a recorder (dimensions:  $5.5 \times 2 \times 9$  cm; weight: 0.1 kg) worn with a wallet on the ankle. The time series of stride interval and its two subphases (stance interval and swing interval) from the foot switches were digitized by an on-board analog-to-digital converter at the sampling rate of 300 Hz with 12-bit resolution per sample. For more details about the data acquisition system and the experimental protocol, readers are referred to Hausdorff et al. [12].

### 2.2 Outlier processing

With the aim to minimize the start-up effects during recording, the samples of each gait rhythm time series recorded in the first 20 s were removed before the gait rhythm analysis (see Fig. 1), which was the same as implemented in the previous studies of Hausdorff et al. [12]. In the gait assessment experiment described above, the subjects were instructed to walk up and down the straight hallway without stopping, unless at the end of the hallway they had to turn around [12]. Therefore, the stride-interval samples recorded during the walking turns (regarded as outliers) should be with large values. According to the well-known "three-sigma rule" [10], about 99.7% of the normally distributed probability values falls in the 3-SD distance from the mean. The stride-interval outliers should take place with a probability of

<sup>1</sup> Online available at <http://www.physionet.org/physiobank/database/gaitnidd/>

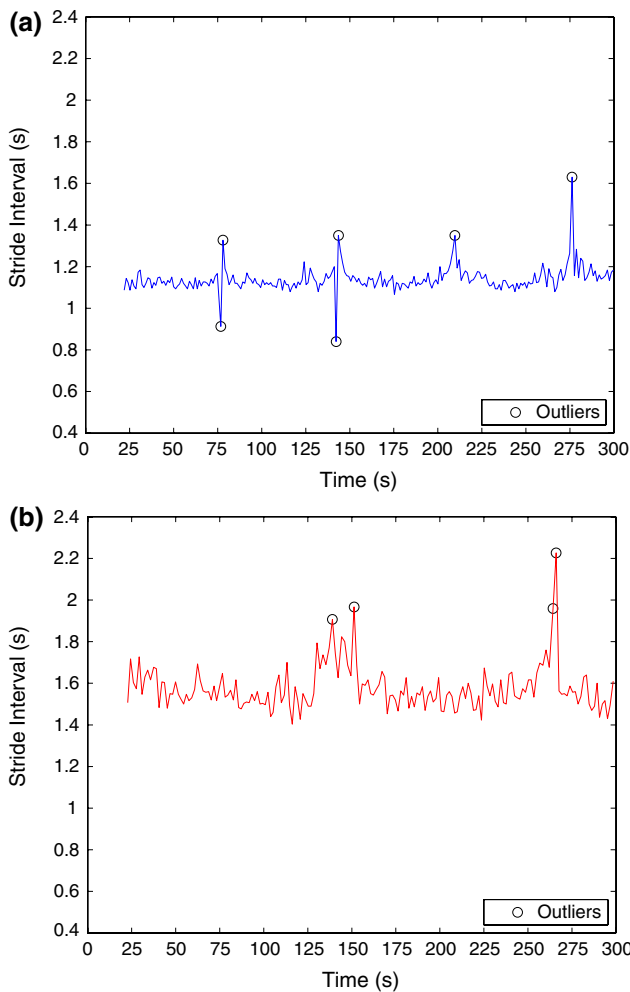


**Fig. 1** Examples of the raw stride-interval time series **a** of a 74-year-old healthy control male subject, and **b** of a 43-year-old male subject with amyotrophic lateral sclerosis (pathological duration of 17 months). Outliers (marked with *circles*) represent the data samples that were 3 standard deviations (SDs) greater or less than the median value over the entire stride-interval time series

occurrence lower than 0.3%, and their values are considered to be 3-SDs greater or less than the median value<sup>2</sup> over the entire stride-interval time series. In the present study, the stride-interval outliers were replaced with the median value of the stride-interval time series from one subject to another. For each subject, the outliers of swing interval (a subphase of stride interval) were also replaced with the median swing-interval value in the time series, before the swing-interval fluctuation analysis described in Sect. 2.3.1. The results of outlier processing are presented in Sect. 3.1.

<sup>2</sup> The median value was used instead of the mean of the stride-interval time series since some outliers were with very large values and might affect the mean of the entire time series.

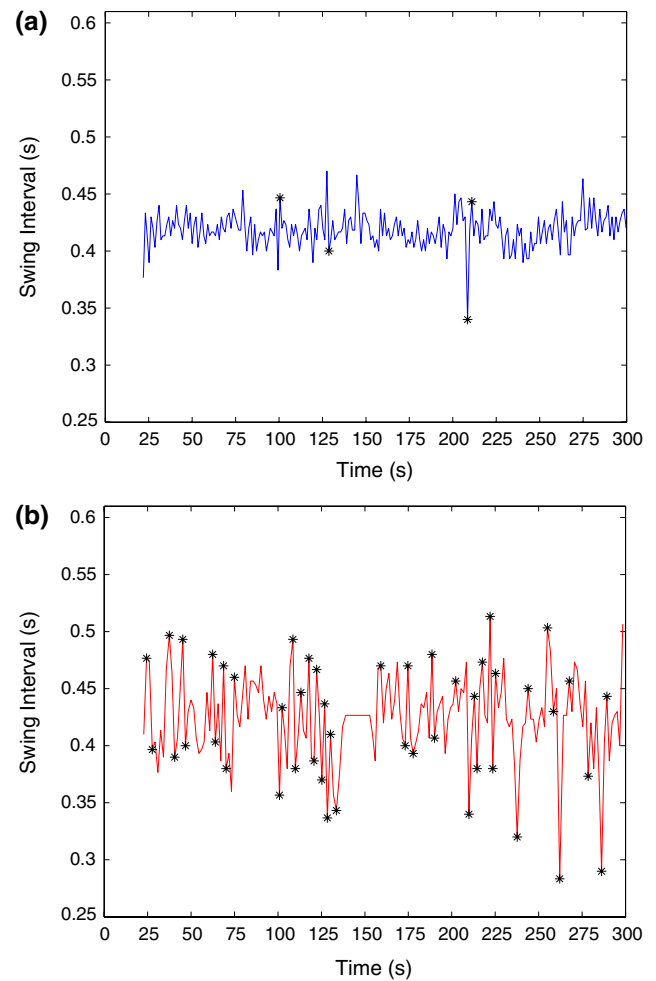


**Fig. 2** Examples of the raw swing-interval time series **a** of a 74-year-old healthy control male subject, and **b** of a 43-year-old male subject with amyotrophic lateral sclerosis (disease duration of 17 months). Significant swing-interval turns detected have been marked with *asterisks*. The swing-interval samples at the precise moments in time when the stride-interval outliers occurs have been removed

### 2.3 Extraction of gait rhythm features

#### 2.3.1 Swing-interval turns count

Figure 2a illustrates an example of the effects of ALS on the outlier-processed swing-interval dynamics in the time domain. It can be observed that the swing-interval time series of both the healthy CO and ALS subjects fluctuated around 0.42 s, but the amplitude of swing interval was dramatically altered in ALS, as shown in Fig. 2b. In order to characterize the degree of fluctuation in the swing-interval time series, we considered the signal turns count method [24].

The signal turns count method was first used by Willison [32] for analysis of electromyographic (EMG) signals. The experimental results suggested that the EMG signal

recorded from the patient with a myopathy usually provides more signal turns than the signal of a normal subject at a comparable level of volitional effort [32]. The recent study of Rangayyan and Wu [25] on the knee-joint vibroarthrographic (VAG) signal analysis showed that the number of VAG signal turns may serve as a promising indicator for screening of knee-joint disorders. These successful biomedical applications demonstrated that the signal turns count parameter can be used to measure the signal variability. In the present study, we would like to apply the signal turns count method to conduct a pilot study on the swing-interval fluctuations in ALS.

According to Rangayyan [24], a data sample can be identified as a “turn” in the signal if it satisfies the following two conditions at the same time: (1) it represents an alteration in direction in the signal, i.e., a change in the sign of the derivative (from positive to negative, or vice versa); (2) the difference between its amplitude and that of the preceding sample is over a certain threshold. The total number of the signal turns in the time series can be used to present the degree of fluctuation dynamics or variability of the signal. For the present study, the detection of the signal turns in a  $N$ -length swing-interval time series,  $\{x_n\}$ ,  $n = 1, 2, \dots, N$ , can be expressed as

$$x_n \text{ is a signal turn, if } \begin{cases} (x_n - x_{n-1})(x_{n+1} - x_n) < 0, \\ |x_{n+1} - x_n| \geq h, \quad 2 \leq n \leq N - 1, \end{cases} \quad (1)$$

where  $h$  denotes the threshold. Then, the swing-interval turns count (SWITC) parameter, i.e., the number of swing-interval turns, was used to measure the swing-interval fluctuations in ALS, and also to derive the gait patterns for classification purpose. The optimal choice of  $h$  and the results of the SWITC feature for ALS gait analysis are presented in Sect. 3.2.

### 2.3.2 Averaged stride interval

As suggested by Hausdorff et al. [12], the stride interval is much longer in patients with ALS, compared with that of healthy adults. Hence, in addition to the SWITC parameter, the averaged stride interval (ASI) was considered as the other dominant feature to characterize the ALS gait patterns. In the present study, the stride interval of each subject was averaged over the outlier-processed time series. The statistics and the results of discriminant significance of the ASI are presented in Sect. 3.2.

## 2.4 Pattern classification

Machine learning tools, such as support vector machine (SVM), are useful for human gait analysis. In the study of Lau et al. [18], five different walking conditions were

successfully classified by the SVM based on the kinematic data obtained in the pre-swing phase. In the present study we applied the linear and nonlinear classifiers to distinguish the gait patterns of ALS patients from those of healthy controls. The Fisher’s linear discriminant analysis (FLDA) [7] was used as the linear classifier, and the least squares support vector machine (LS-SVM) proposed by Suykens et al. [30] was implemented for the nonlinear classification.

The LS-SVM is a reformulation to the standard SVM proposed by Cortes and Vapnik [6]. Similar to the standard SVM, the LS-SVM is also a type of kernel-based feed-forward network, the learning of which follows the principle of structural risk minimization [31]. In order to optimize the model parameters of the LS-SVM, a subset of the representative training data is selected to serve as the support vectors, which are considered to be the most informative for the classification task. By choosing the nonlinear inner-product kernels in the network, the LS-SVM is able to perform the same function as the polynomial learning machine, radial-basis function network, or multi-layer perceptron with a single hidden layer [16]. The major difference between the LS-SVM and the standard SVM is that the learning of the LS-SVM is implemented by minimizing a regularized least-squares cost function with equality constraints, under the Karush–Kuhn–Tucker (KKT) condition [23]. Thus, the LS-SVM works efficiently with an improvement of moderate complexity. For more details of theoretical framework of the LS-SVM, readers are referred to the book authored by Suykens et al. [30].

In order to determine the kernel function suited for the classification of gait patterns, we implemented the LS-SVM using the polynomial, sigmoid, and Gaussian kernels, one by one specified with different values of model parameters, and then tested each LS-SVM with the leave-one-out (LOO) cross-validation method. Receiver operating characteristic (ROC) curves were generated for both the FLDA and the LS-SVM with the software ROCKIT<sup>3</sup> provided by the University of Chicago [20]. The area ( $A_z$ ) under the ROC curve was derived to serve as a measure of the overall diagnostic performance in each classification experiment. By checking the classification accuracy and the ROC curve provided by the LS-SVM with different kernels (along with their optimal model parameters), we found that the best classification performance can be achieved by the LS-SVM with the sigmoid kernels and with the zero bias and unity scale parameters for the sigmoid-kernel function, i.e.,

$$\kappa(\mathbf{f}_i, \mathbf{f}_j) = \tanh(\mathbf{sf}_i^T \mathbf{f}_j + b^2), \quad (2)$$

<sup>3</sup> Online available at [http://www-radiology.uchicago.edu/krl/KRL\\_ROC/software\\_index6.htm](http://www-radiology.uchicago.edu/krl/KRL_ROC/software_index6.htm)

where the scale parameter  $s = 1$ , the bias  $b = 0$ , and  $\mathbf{f}_i$  presents the ASI-SWITC feature vector of the  $i$ th subject. The regularization parameter equal to 5 can provide the sigmoid-kernel-based LS-SVM with the highest classification accurate rate, together with the largest  $A_z$  value under the ROC curve, which were better than the results obtained by the LS-SVM with polynomial or Gaussian kernels. The details of the classification performance of the FLDA and the sigmoid-kernel-based LS-SVM are presented in Sect. 3.3.

### 3 Results

#### 3.1 Outlier processing results

Figure 1 shows the detected outliers (marked as *circles*), i.e., the stride-interval samples at 76.8, 78, 142.2, 143.5, 209.7, and 276.3 s in Fig. 1a for a 74-year-old healthy control (CO) subject and at 139, 151.3, 264.3, and 266.1 s in Fig. 1b for a 43-year-old subject with amyotrophic lateral sclerosis (ALS), respectively. With the annotations of the stride-interval outliers, for each subject, the swing-interval outliers associated with the walking turns at the end of the hallway were also replaced with the median value of the corresponding swing-interval time series.

#### 3.2 Feature extraction results

In order to determine the optimal threshold  $h$  for the feature of swing-interval turns count (SWITC), the value of  $h$  was varied over the range from 0.01 to 0.1 s, increased by a step of 0.01 s. Table 1 provides the mean and SD values of the

**Table 1** Mean and standard deviation (SD) values of the swing-interval turns count for 16 healthy control (CO) subjects and 13 patients with amyotrophic lateral sclerosis (ALS)

Threshold (s)	Swing-interval turns count (mean ± SD)		<i>p</i> -value
	CO	ALS	
0.01	118.5 ± 18.5	101.4 ± 22.9	0.0343
0.02	73.9 ± 26.8	81.8 ± 20	0.3867
0.03	38.2 ± 24.7	63.2 ± 23.3	0.0098
0.04	20.1 ± 17.6	47 ± 25.5	0.0023
0.05	10 ± 9.1	35.2 ± 24.6	0.0007
0.06	4.4 ± 4.3	28.4 ± 22	0.0002
0.07	2.9 ± 3.2	22 ± 18.1	0.0003
0.08	2.2 ± 2.4	18.2 ± 16.4	0.0006
0.09	1.6 ± 1.7	13.9 ± 13.7	0.0014
0.1	1.3 ± 1.4	11.3 ± 11.8	0.0023

Statistical significance of separability (in terms of *p*-value) was obtained with the Student’s *t*-test

SWITC detected with the threshold at different levels for the groups of healthy controls and ALS subjects. It can be observed that the SWITC exhibited a monotonically decreasing relationship with the threshold, especially with the highest threshold (0.1 s), few samples were identified as signal turns in most of the swing-interval time series of the healthy CO subjects. We used the Student’s *t*-test [10] to evaluate whether or not the mean value of the SWITC parameter associated with the healthy CO subjects was significantly different from that of the ALS patients. According to the *p*-values listed in Table 1, the SWITC parameter possessed a significant difference ( $p < 0.01$ ) between the healthy CO subjects and the ALS patients, when the threshold was over 0.03 s. Meanwhile, the mean values of the SWITC for the ALS patients were larger than those of the healthy CO subjects, which confirms the hypothesis presented in Sect. 1. In addition, we can observe that *p*-value was monotonically decreasing until reaching a minimum (0.0002), and then monotonically increasing, when  $0.03 \leq h \leq 0.1$  s. Thus, we chose  $h = 0.06$  s that provided the SWITC parameter with the lowest *p*-value (i.e., the highest degree of separability) to derive a dominant feature for further pattern classifications. Figure 2 shows the swing-interval turns detected with the threshold  $h = 0.06$  s for a healthy elderly subject and an ALS patient, respectively. It can be observed that the ALS patient possessed a larger number of swing-interval turns than the healthy elderly subject.

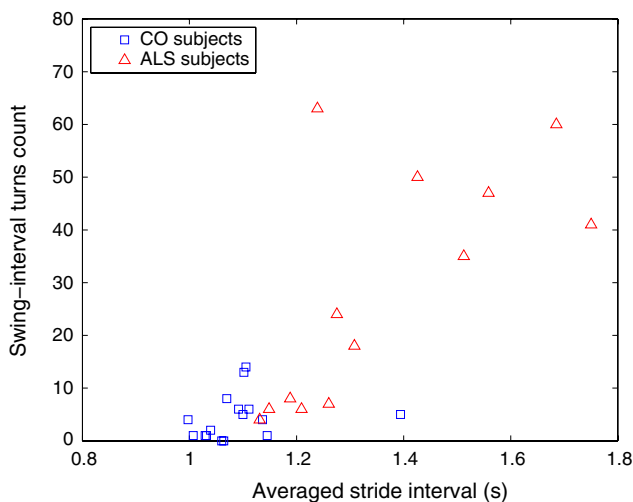
With regard to the feature of averaged stride interval (ASI), the group of ALS patients possessed a mean value of 1.36 s (SD: 0.21 s), which was much larger than the result of the healthy CO group (mean: 1.09 s, SD: 0.09 s). The *p*-value of the ASI feature evaluated with the Student’s *t*-test was  $7 \times 10^{-5}$  ( $p < 0.0001$ ), which indicated the significance of separability between the healthy CO subjects and the ALS patients.

Figure 3 draws in the ASI-SWITC feature space, the gait patterns associated with the healthy CO and ALS subjects using scatter markers of *squares* and *triangles*, respectively. For the healthy CO subjects, it can be observed that the SWITC values were smaller than 20, and the ASI values congregated in the range from 0.9 to 1.2 s, except for one healthy elderly subject who possessed an ASI value of 1.39 s. On the other hand, the ALS patterns were dispersed in a larger area of the ASI-SWITC feature plane.

#### 3.3 Classification results

As described in Sect. 2.4, the linear and nonlinear classification experiments were tested with the leave-one-out (LOO) cross-validation method. In our experiments, the performance of a classifier is presented in terms of overall accurate rate (in percentage) and the area ( $A_z$ ) under the





**Fig. 3** Scatter plot of the gait patterns of the healthy control (CO) subjects, marked as *squares*, and of the subjects with amyotrophic lateral sclerosis (ALS), marked as *triangles*, in the two-dimensional feature space. The gait patterns were characterized by the features of averaged stride interval and swing-interval turns count

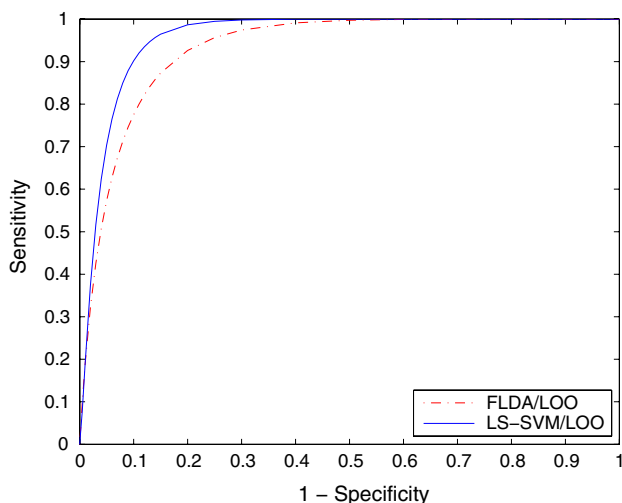


**Fig. 4** Plots of receiver operating characteristic (ROC) curves obtained with the Fisher's linear discriminant analysis (*dash-dot line*) and the sigmoid-kernel-based least squares support vector machine (*solid line*). The leave-one-out (LOO) cross-validation method was applied to evaluate the classification performance for the Fisher's linear discriminant analysis (labeled as FLDA/LOO) and the sigmoid-kernel-based least squares support vector machine (labeled as LS-SVM/LOO), respectively. The corresponding areas ( $A_z$ ) under the ROC curves for the FLDA/LOO and the LS-SVM/LOO were 0.9315 (standard error, SE: 0.0470) and 0.9629 (SE: 0.0385), respectively

receiver operating characteristic (ROC) curve. The Fisher's linear discriminant analysis evaluated with the LOO method (labeled as FLDA/LOO) provided an overall accurate rate of 82.76%, which was acceptable in practice, whereas the sigmoid-kernel-based least squares support vector machine evaluated with the LOO method (labeled as

LS-SVM/LOO) can even reach a higher overall accurate rate (89.66%), with an improvement of 6.9% correct classifications. The LS-SVM/LOO provided the overall diagnostic performance with the  $A_z$  of 0.9629 (standard error, SE: 0.0385), which was better than the ROC result of the FLDA/LOO ( $A_z$ : 0.9315, SE: 0.0470).

The ROC curves obtained with the FLDA/LOO and the LS-SVM/LOO are shown in Fig. 4, from which we can observe that the ROC curve of the LS-SVM/LOO was consistently over that of the FLDA/LOO. Such results indicated that the performance of the LS-SVM/LOO (nonlinear classification) was superior to that of the FLDA/LOO (linear classification), which demonstrated the advantages of the least squares support vector machine for ALS gait analysis. On the other hand, although the FLDA/LOO cannot provide the classification performance as good as the LS-SVM/LOO, the  $A_z$  value produced with the linear classification was still over 0.93, which implies that the ASI and SWITC features may be positively considered as dominant indicators for analysis of ALS gait patterns.

#### 4 Discussion

In the outlier processing procedure, which was implemented before the signal turns count method, we did not simply removed the samples associated with the walking turns, but replaced them with the median value of the time series instead. It is worth noting that such a procedure would not affect the results of the signal turns count detection, as those swing-interval outliers were replaced with the identical median value in a time series, and there was no change in amplitude during the walking turns (visible in Fig. 2b in the duration from 139 to 151.3 s).

Since the total number of swing-interval turns in the time series was counted up during the 5-min monitoring period, the final count would depend upon the number of strides, i.e., if more steps a subject took, the more opportunities a swing-interval turn could occur. From Fig. 1, we may observe that the healthy subject reached the end of the hallway for four times and the ALS patient only did twice. It can be inferred that the walking speed of the healthy subject was faster than that of the ALS patient, and more strides should be taken by the healthy subject within 5 min. Based on such an inference, the healthy subject should normally produce more swing-interval turns, due to a larger number of strides taken. However, from Fig. 2, the number of swing-interval turns count for the healthy subject was much less than that of the ALS patient, which implies that even the gait speed of the ALS patient was slower than the healthy subject, as observed by Hausdorff et al. [12], the swing-interval time series recorded with the same monitoring period still exhibited a much higher degree of fluctuations for the ALS patient.

The stride interval of healthy elderly subjects is usually longer than healthy adults. In order to study whether or not the stride interval of patients with ALS is still longer than that of healthy elderly subjects, we also used the Student's *t*-test to evaluate the ASI values between the healthy elderly subjects (age >60 years) and the ALS patients. The *p*-value obtained was 0.0454 ( $p < 0.05$ ), therefore, the ASI feature was considered to be reliable in the present study to derive the ALS gait patterns.

Computer-aided analysis of the gait rhythm of patients with neurodegenerative symptoms by using signal processing and machine learning techniques may provide important diagnostic information that can be used to distinguish particular disorders of motor or sensory function, or even specific neurodegenerative diseases. In this article, we studied two dominant features, i.e., the averaged stride interval and swing-interval turns count, extracted from the outlier-processed gait dynamics time series, and then distinguished the gait patterns of patients with amyotrophic lateral sclerosis from those of healthy controls by using the linear and nonlinear classifiers. The results obtained in our experiments demonstrated the advantages of the averaged stride interval and swing-interval turns count features, along with the merits of the least squares support vector machine, for computer-aided analysis of the gait in amyotrophic lateral sclerosis.

**Acknowledgments** This study was supported, in part, by the funds provided by the Natural Sciences and Engineering Research Council of Canada (NSERC) and the Canada Research Chairs Program.

## References

- Akay M, Sekine M, Tamura T, Higashi Y, Fujimoto T (2003) Unconstrained monitoring of body motion during walking. *IEEE Eng Med Biol Mag* 22(3):104–109
- Akay M, Sekine M, Tamura T, Higashi Y, Fujimoto T (2004) Fractal dynamics of body motion in post-stroke hemiplegic patients during walking. *J Neural Eng* 1(2):111–116
- Brooks BR (1996) Natural history of ALS: symptoms, strength, pulmonary function, and disability. *Neurology* 47(4 Suppl 2):S71–S81
- Brown RH (1997) Amyotrophic lateral sclerosis: insights from genetics. *Arch Neurol* 54(10):1246–1250
- Brown RH, Meininger V, Swash M (1999) Amyotrophic lateral sclerosis. Martin Dunitz Publishers, London, UK
- Cortes C, Vapnik VN (1995) Support-vector networks. *Mach Learn* 20(3):273–297
- Duda RO, Hart PE, Stork DG (2001) Pattern classification, 2nd edn. Wiley, New York, NY
- Emborg J, Spaich EG, Andersen OK (2009) Withdrawal reflexes examined during human gait by ground reaction forces: site and gait phase dependency. *Med Biol Eng Comput* 47(1):29–39. doi: [10.1007/s11517-008-0396-x](https://doi.org/10.1007/s11517-008-0396-x)
- Goldfarb BJ, Simon SR (1984) Gait patterns in patients with amyotrophic lateral sclerosis. *Arch Phys Med Rehab* 65(2):61–65
- Hahn GJ, Shapiro SS (1994) Statistical models in engineering. Wiley, Hoboken, NJ
- Hausdorff JM, Alexander NB (2005) Gait disorders: evaluation and management. Informa Healthcare, New York, NY
- Hausdorff JM, Lertratanakul A, Cudkowicz ME, Peterson AL, Kaliton D, Goldberger AL (2000) Dynamic markers of altered gait rhythm in amyotrophic lateral sclerosis. *J Appl Physiol* 88(6):2045–2053
- Hausdorff JM, Mitchell SL, Firtion R, Peng CK, Cudkowicz ME, Wei JY, Goldberger AL (1997) Altered fractal dynamics of gait: reduced stride-interval correlations with aging and Huntington's disease. *J Appl Physiol* 82(1):262–269
- Hausdorff JM, Peng CK, Ladin Z, Wei JY, Goldberger AL (1995) Is walking a random walk? Evidence for long-range correlations in stride interval of human gait. *J Appl Physiol* 78(1):349–358
- Hausdorff JM, Purdon PL, Peng CK, Ladin Z, Wei JY, Goldberger AL (1996) Fractal dynamics of human gait: stability of long-range correlations in stride interval fluctuations. *J Appl Physiol* 80(5):1448–1457
- Haykin S (1998) Neural networks: a comprehensive foundation, 2nd edn. Prentice Hall PTR, Englewood Cliffs, NJ
- Hirano A (1996) Neuropathology of ALS: an overview. *Neurology* 47(4 Suppl 2):63–66
- Lau HY, Tong KY, Zhu HL (2008) Support vector machine for classification of walking conditions using miniature kinematic sensors. *Med Biol Eng Comput* 46(6):563–573. doi: [10.1007/s11517-008-0327-x](https://doi.org/10.1007/s11517-008-0327-x)
- Leigh PN, Meldrum BS (1996) Excitotoxicity in ALS. *Neurology* 47(6 Suppl 4):221–227
- Metz C, Herman B, Shen J (1998) Maximum-likelihood estimation of ROC curves from continuously-distributed data. *Stat Med* 17(9):1033–1053
- Meyer AR, Wang M, Smith PA, Harris GF (2007) Modeling initial contact dynamics during ambulation with dynamic simulation. *Med Biol Eng Comput* 45(4):387–394. doi: [10.1007/s11517-007-0166-1](https://doi.org/10.1007/s11517-007-0166-1)
- Moody GB, Mark RG, Goldberger AL (2001) PhysioNet: a web-based resource for the study of physiologic signals. *IEEE Eng Med Biol Mag* 20(3):70–75
- Nash SG, Sofer A (1995) Linear and nonlinear programming. McGraw-Hill, Columbus, OH
- Rangayyan RM (2002) Biomedical signal analysis: a case-study approach. IEEE and Wiley, New York, NY
- Rangayyan RM, Wu YF (2009) Analysis of vibroarthrographic signals with features related to signal variability and radial-basis functions. *Ann Biomed Eng* 37(1):156–163. doi: [10.1007/s10439-008-9601-1](https://doi.org/10.1007/s10439-008-9601-1)
- Ropper AH, Brown RH (2005) Adams and Victor's principles of neurology, 8th edn. McGraw-Hill, New York, NY
- Sekine M, Akay M, Tamura T, Higashi Y (2004) Fractal dynamics of body motion in patients with Parkinson's disease. *J Neural Eng* 1(1):8–15
- Sekine M, Tamura T, Akay M, Fujimoto T, Togawa T, Fukui Y (2002) Discrimination of walking patterns using wavelet-based fractal analysis. *IEEE Trans Neural Syst Rehab Eng* 10(3):188–196. doi: [10.1109/TNSRE.2002.802879](https://doi.org/10.1109/TNSRE.2002.802879)
- Sharma KR, Kent-Braun JA, Majumdar S, Huang Y, Mynhier M, Weiner MW, Miller RG (1995) Physiology of fatigue in amyotrophic lateral sclerosis. *Neurology* 45(4):733–740
- Suykens JAK, Van Gestel T, De Brabanter J, De Moor B, Vandewalle J (2002) Least squares support vector machines. World Scientific Publishing, Singapore
- Vapnik VN (1998) Statistical learning theory. Wiley, New York, NY
- Willison RG (1964) Analysis of electrical activity in healthy and dystrophic muscle in man. *J Neurol Neurosurg Psychiatry* 27(5):386–394